Sensitive profiling of chemically diverse bioactive lipids[S]

Guanghou Shui,[1],* Anne K. Bendt,[1],* Kevin Pethe,[†] Thomas Dick,[†] and Markus R. Wenk[2],*,§

Yong Loo Lin School of Medicine,* National University of Singapore, Department of Biochemistry, Singapore, 117597; Novartis Institute for Tropical Diseases,[†] Singapore, 138670; and Department of Biological Sciences,[§] Singapore, 117597

Abstract Here, we present an improved method for sensitive profiling of lipids in a single high-performance liquid chromatography-electrospray ionization-quadrupole time of flight mass spectrometry experiment. The approach consists of *i*) sensitive isocratic elution, which takes advantage of C18 column material that is resistant to increased pH values induced by piperidine, *ii*) chemometric alignment of mass spectra followed by differential analysis of ion intensities, and *iii*) semiquantitative analysis of extracted ion chromatograms of interest. A key advantage of this method is its wide applicability to extracts that harbor lipids of considerable chemical complexity. The method allows qualitative and semiquantitative analysis of fatty acyls, glycerophospholipids (such as glycerophosphatidylinositols, glycerophosphatidylserines, and glycerophosphatidylcholines in brain extracts), phosphatidylinositol mannosides, acylated glycerophospholipids, sphingolipids (including ceramides and gangliosides in brain extracts), and, for the first time with ESI, prenols and mycolic acids (MAs). MAs are targets in antimycobacterial therapy, and they play an important immunomodulatory role during host-pathogen interactions. We compared high-resolution mass spectra of MAs derived from *Mycobacterium bovis* Bacille Camette-Guérin during entry into nonreplicative conditions induced by oxygen deprivation (hypoxic dormancy). Although the overall composition is not drastically altered, there are pronounced differences in individual MAs. α-MAs accumulate during entry into dormancy, whereas a subpopulation of keto-MAs is almost entirely eliminated. This effect is reversed upon resuscitation of dormant mycobacteria.[JLR] These results provide detailed chemical information with relevance to drug development and immunobiology of mycobacteria.— Shui, G., A. K. Bendt, K. Pethe, T. Dick, and M. R. Wenk. **Sensitive profiling of chemically diverse bioactive lipids.** *J. Lipid Res.* 2007. **48:** 1976–1984.

Advances in MS have created powerful new avenues for the measurement of global changes in the cellular lipid inventory. ESI mass spectrometry has been successfully used to measure lipids in various cell types (1, 2). A major advantage of these methods is that they generally only require a single analytical step (i.e., mass spectrometric detection without prior sample derivatization or separation). In addition, detailed studies of fragmentation pathways of phospholipids (3, 4) spurred subsequent development of selective tandem mass spectrometry methods that are now widely used for the analysis of well-characterized and abundant phospholipids and sphingolipids (5, 6).

Although such methods work relatively well for the analysis of abundant lipids, they are less well suited for the detection, characterization, and quantification of lipids that *i*) are less abundant and *ii*) have more complicated chemical compositions. HPLC is an ideal upfront separation before ionization by ESI and detection by MS. Indeed, LC-MS is now commonly used for the analysis of sphingolipids from complex mixtures (6, 7). Two-dimensional analysis of phospholipids using LC-MS is less well established, in part because of the success of the tandem mass spectrometry approaches mentioned above. Capillary HPLC in combination with ESI-MS was recently used to provide two-dimensional maps of major phospholipids (8), yet unusual or minor lipid components are not easily covered because of their low limit of detection. More recently, a robust method, based on isocratic elution followed by automated detection and quantification of molecular species of the major lipid classes, was described (9). Ultraperformance liquid chromatography coupled with mass spectrometry has also been developed for the rapid separation and analysis of various lipids (10).

"Nontargeted" readouts (i.e., detection that does not require prior knowledge of lipid chemistry and identity) are desirable in many applications in the life sciences. Here, we emphasize the importance of such nontargeted lipid profiling and describe a novel method that allows the detection and quantification of a wide variety of lipid

Abbreviations: BCG, Bacille Camette-Guérin; COW, correlation-optimized warping; MA, mycolic acid; PIP, phosphatidylinositol polyphosphate; Q-TOF, quadrupole/time of flight.

[1] G. Shui and A. K. Bendt contributed equally to this work.
[2] To whom correspondence should be addressed.
    e-mail: bchmrw@nus.edu.sg
[S] The online version of this article (available at http://www.jlr.org) contains supplementary data in the form of one figure.

classes. HPLC coupled with high-resolution quadrupole/ time of flight Q-TOF) MS provides the basis for this method. Ion suppression is reduced by the use of piperidine and column materials that can withstand high pH values. This method is an excellent screening tool for the comparison of "paired samples," such as extracts from "control" versus "treated" tissues/cells (11). We use this method in a comparative study of lipid extracts derived from mycobacteria grown under different physiological conditions to compare the levels of complex mycolic acids (MAs) and their derivatives.

MATERIALS AND METHODS

Chemicals and materials

Lipid standards and brain polar lipids (bovine) were purchased from Avanti Polar Lipids (Alabaster, AL). All solvents were HPLC-grade and were purchased from Merck (Merck Pte., Ltd., Singapore). Piperidine was purchased from Sigma-Aldrich (Steinheim, Germany). Deionized water was obtained from a Milli-Q water system (Millipore, Milford, MA).

Lipid standards

Individual phospholipid samples were freshly prepared from dilutions of stock solutions. Brain polar lipids were diluted to a final concentration of 125 μg/ml with chloroform-methanol (1:1, v/v) for comparative analysis with or without 30 mM piperidine (added from a 300 mM stock in water) for MS and LC-MS analysis. Brain polar lipids were spiked with 0, 1, 2, or 4 μg/ml synthetic POPC for the determination of standard curves. In addition, different volumes of the lipid standards C19:0 ceramide (24 μg/ml), 1-palmitoyl-2-oleoyl-sn-glycero-3-phosphocholine (6 μg), and 1,1′,2,2′-tetralinoleoyl cardiolipin (100 μg/ml) were spiked into 100 μl (125 μg/ml) of brain polar lipids for LC-MS assay. MA standards from *Mycobacterium tuberculosis* were purchased from Sigma. Total lipid extracts from *M. tuberculosis* were kindly provided by Dr. John T. Belisle (Colorado State University, under TB contract number SG 0057). Dilution series were prepared (ranging from 10 to 250 μg/ml MAs) to assess the linearity of ion responses.

Mycobacterial cultures and lipid extracts

The attenuated vaccine strain *Mycobacterium bovis* Bacille Camette-Guérin (BCG) Pasteur (American Type Culture Collection 35734) was used in all experiments and cultivated in Dubos Tween-albumin broth (Difco Laboratories, Ltd., West Molesey, United Kingdom), complemented with 0.05% (v/v) Tween 80 (Sigma). For Wayne dormancy cultures, a self-generated gradual oxygen depletion was achieved by incubating the obligate aerobic cells in sealed screw-capped glass tubes (20 mm × 125 mm) in a final volume of 17 ml, with a starting optical density at 600 nm of 0.005, at 37°C under constant stirring at 180 rpm on magnetic stirring platforms (12). The redox indicator dye methylene blue was used to monitor decreasing levels of oxygen. Extended incubation resulted in oxygen depletion, when mycobacterial growth ceased and cells entered a state of nonreplicative persistence, also referred to as "dormancy." These dormant bacteria were harvested after 20 days of incubation. For the resuscitation of hypoxia-induced dormant cells, the incubation tubes containing dormant cells were opened to allow aeration of the medium. Bacteria resumed growth after a lag phase of 1 day and were

harvested after a resuscitation period of 5 days. Aerated stationary phase cells were incubated in the same glass tubes under identical growth conditions but covered only with loose caps to allow constant aeration of the culture. Aerated bacterial cultures became stationary after 10 days of incubation and were harvested.

For total lipid extraction, mycobacterial cells were harvested in Teflon-fluorinated ethylene propylene tubes (Nalgene, Rochester, NY). Cell pellets were resuspended in 5 ml of chloroform-methanol (2:1, v/v) and incubated overnight at 4°C under constant shaking at 200 rpm. Separation of aqueous and organic phases was performed by the addition of 3 ml of deionized water and 20 min of centrifugation at 4,000 rpm. The clean organic phase was collected into a fresh glass vial, and lipids were dried under a gentle stream of nitrogen. The white intermediate layer ("delipidated cells") was used for subsequent alkaline hydrolysis (see below). Dried total lipid films were stored at −20°C until further use.

To release esterified MAs from the cell wall by alkaline hydrolysis, the defatted cells resulting from chloroform-methanol extraction were washed once with deionized water and dried. Alkaline hydrolysis was performed by adding 1 ml of 1 M KOH/ methanol for 2 h at 80°C at 600 rpm. Extracts were cooled to room temperature and acidified to pH ∼ 5 with HCl. Liberated MAs were extracted twice with 1 ml of diethyl ether. The ether phase were washed once with deionized water and dried.

MS and LC-MS

ESI-MS was performed on a Waters Micromass Q-TOF micromass spectrometer with an upfront Waters CapLC inlet (Waters Corp., Milford, MA). The capillary voltage and sample cone voltage were maintained at 3.0 kV and 50 V, respectively. The source temperature was 80°C, and the desolvation temperature was set at 250°C. Mass spectra were acquired in the negative ion mode with an acquisition time of 3 min. Chloroform-methanol (1:1, v/v) at a flow rate of 15 μl/min was used as the mobile phase. Typically, 2 μl of sample without piperidine was injected for analysis.

In LC-MS experiments, a Waters XTerra column (1 mm × 150 mm) was used for the separation of lipids. Chloroform-methanol (1:1, v/v) with 5% 300 mM piperidine (final concentration,15 mM) was used as the mobile phase for isocratic elution. For separation of brain polar lipids, a flow rate of 8 μl/min was used for a rapid analysis of lipids (∼20 min). For separation of mycobacterial lipids, a flow rate of 10 μl/min was used in a total run time of 85 min. The capillary voltage was set at 3.0 kV. The sample cone voltages were maintained at 50 V for brain polar lipids and 65 V for MAs. The column eluent was introduced into the standard electrospray source of a Waters Micromass Q-TOF micromass spectrometer operated in the negative ion mode. The mass spectrum was acquired from *m/z* 400 to 1,000 with a frequency of 1 scan/1 s for brain polar lipids and from *m/z* 500 to 1,700 with a frequency of 1 scan/1.6 s for mycobacterial samples. Typically, 2 μl of sample with 5% 300 mM piperidine was injected for analysis.

Data processing and comparative analysis

Lipid chromatograms were combined to generate combined spectra and a corresponding spectrum list using MassLynx 4.0 (Waters Corp.). The data were next migrated to MatLAB (MathWorks, Inc., Natick, MA) for alignment of spectra using correlation-optimized warping (COW) (13) (**Fig. 1**). COW was originally used to align chromatographic profiles with drifts in elution times. The method is based on piecewise linear stretching and compression along the time axis of one of the profiles, using another profile as a reference (14). Most importantly, the peak
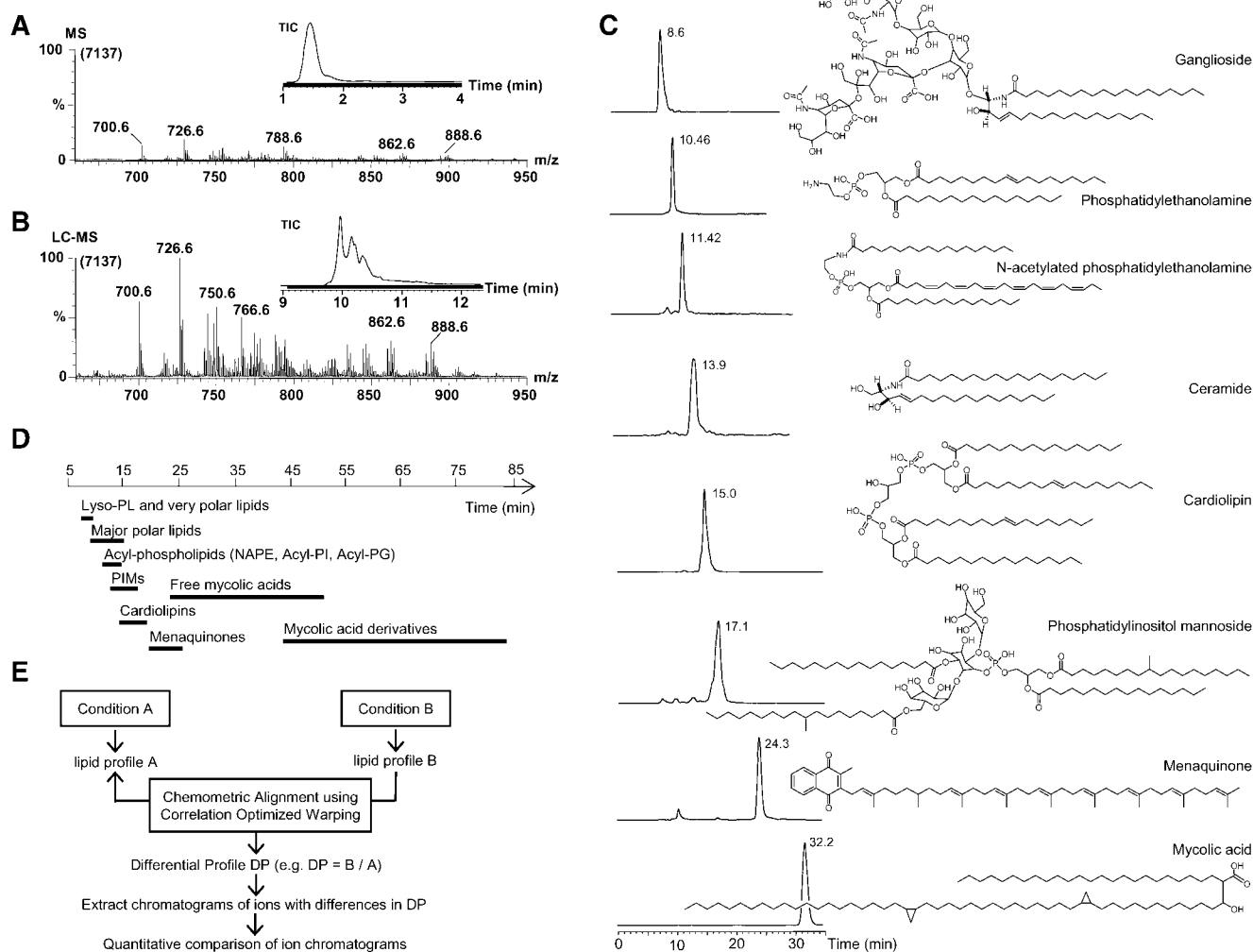
Fig. 1. Enhanced sensitivity HPLC-MS profiling of chemically diverse lipids in complex mixtures. A: MS detection of total brain lipids without upfront chromatography [the inset displays the total ion chromatogram (TIC) bypassing the column]. B: MS detection of total brain lipids with upfront chromatography and piperidine as an signal enhancer (the inset displays the total ion chromatogram of HPLC-MS, and the black bar under the total ion chromatogram indicates the elution period for which ion chromatograms were combined to generate the mass spectrum). Chromatographic preseparation leads to substantial gains in sensitivity and aids in the detection of ions that would otherwise be suppressed. C: Representative ion chromatograms of chemically diverse lipids in complex mixtures (data are a compilation of results from several different applications). Polar lipids such as lysophospholipids (not shown) and gangliosides (top) elute within ~10 min, whereas nonpolar compounds such as menaquinones and mycolic acids (MAs) elute at much later time points and are thus separated before mass spectrometric analysis. D: Summary of elution periods of biologically important lipids. NAPE, *N*-acetylated phosphatidylethanolamine; PG, phosphatidylglycerol; PIM, phosphatidylinositol mannoside; PL, phospholipid. E: Cartoon illustrating the general approach for HPLC-MS-based analysis of paired samples. DP, differential profile.

height, shape, and area are largely unaffected by this procedure. We chose one of the spectra from the replicates of the control condition as the reference spectrum against which the other profiles of the other control replicates were warped. This procedure was repeated for spectra originating from the "perturbed" condition (e.g., spiked samples or mycobacterial extracts from dormant cells). The resulting warped profiles were averaged using simple arithmetic. Differential analyses of the MS profiles were next computed, and results are shown as fold differences in absolute and logarithmic values. Ions that showed significant differences between the control and perturbed samples were selected and their chromatograms extracted using MassLynx 4.0 software. Integrated peak areas and/or their normalized values were used for semiquantitative analysis.

RESULTS AND DISCUSSION

Sensitive LC-MS detection of chemically complex lipids

Many cellular phospholipids are effectively ionized and detected by ESI-MS in the negative ionization mode. Even phosphatidylcholine and sphingomyelin, which are more sensitively detected in the positive ionization mode, are readily detectable as their demethylated or chloride-adduct (negative) ions. Therefore, negative ESI mass spectra of crude cellular extract cover all classes of polar phospholipids. Hence, we decided to limit our method to negative ionization, thus simplifying analysis to one polarity. Piperidine, a signal enhancer for polar lipids during

ESI, was found to significantly increase the signal intensities of phosphatidylinositol polyphosphates (PIPs), including PIP and PIP$_2$ (15), which makes direct measurements of PIPs feasible in total lipid mixtures. In addition, piperidine also was an excellent signal enhancer for PIP$_3$ (data not shown). Piperidine has been used in reverse phase as a postcolumn modifier for the detection of glycerophospholipids in the negative ion mode (16). After the addition of piperidine to the mobile phase, the ion responses of all polar lipids tested here were increased by 2- to 10-fold, or even much more for some special lipids such as PIPs (data not shown). Piperidine also enhanced the ion responses for phosphatidylcholine and sphingomyelin by >2-fold (data not shown).

We established conditions that allow the use of piperidine in combination with chromatographic separation. Traditional HPLC methods operate columns (both normal phase and reverse phase) usually in pH ranges of 1–8 and binary gradient mobile phases. As most polar lipids are amphiphilic, they have strong affinities to both reverse and normal stationary phases and often elute as broad peaks. Traditional columns are not suitable for piperidine-containing samples or mobile phases, because piperidine will induce back-pressure from stationary phase degradation and alterations in retention times attributable to the increased pH. To overcome this problem, piperidine was added as a postcolumn modifier in the past (16). Recently, column materials that can withstand high-pH environments became available commercially (e.g., XTerra C18 column; Waters). Piperidine, a heterocyclic organic amine, aids in the deprotonation of lipids and competes for active sites. This leads to a reduction in tailing of polar lipids and an increase in peak symmetry during reverse-phase LC separation. Thus, using piperidine in the mobile phase significantly increases sensitivity.

Using isocratic elution, this new LC-MS approach provides enhanced sensitivity (approximately five times on average) for many if not all lipids from brain compared with analysis without preseparation (Fig. 1A, B). Note that one column has been used under such a high-pH environment for 2 years with very reproducible performance (>500 injections). This method thus combines the advantages of piperidine as a signal enhancer and of chromatographic preseparation, which reduces ion suppression and isobaric interference. Indeed, we found good separation for a diverse array of lipids. Free fatty acids, lysophospholipids, and very polar lipids such as gangliosides elute first, followed by major cellular glycerophospholipids, cardiolipins, and more complicated lipids such as phosphatidylinositol mannoside and nonpolar molecules such as menaquinones, free MAs, and some of their derivatives (Fig. 1C and data not shown). A summary of the approximate elution sequences of a range of chemically diverse lipids is shown in Fig. 1D.

Although reverse-phase LC techniques are not ideal for the separation of lipids into different lipid classes, they are very useful to differentiate according to lipophilicity. For example, using this reverse-phase LC-MS method, we could separate chemically diverse lipids and, for the first time using ESI, detected a number of bioactive lipids such as MAs and menaquinones without the need for any sample prepurification or chemical derivatization. Isobaric and isotopic effects were significantly reduced by chromatographic separation from bulk lipids (Fig. 1D), thus allowing analysis by single stage ESI-MS analysis (Fig. 1C and data not shown). In addition, separation of free fatty
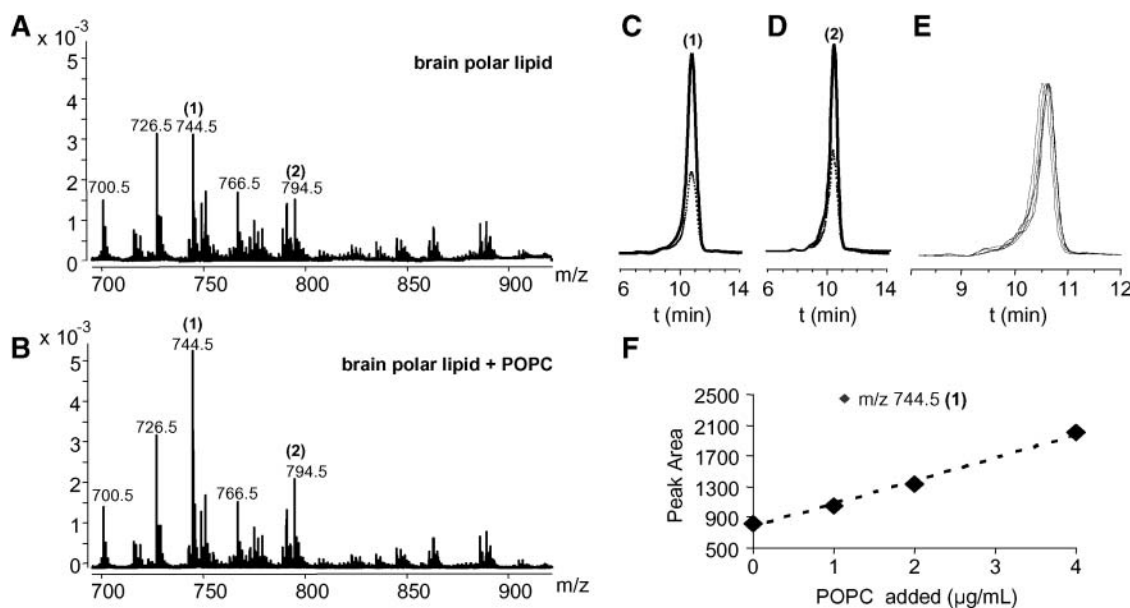

Fig. 2. Method validation. A, B: Comparison of combined spectra from brain polar lipid without (A) and with (B) spiked POPC standard. C, D: Extracted ion chromatograms of m/z 744.5 ([M-15]$^-$; 1) (C) and 794.5 ([M+Cl]$^-$; 2) (D) with (solid peaks) and without (dotted peaks) spiked POPC. E: Within-day retention time reproducibility of POPC (retention time = 10.6 ± 0.1 min; n = 6). F: Standard additions as in A show good linear responses for peak areas of ions at m/z 744.5.

acids from glycerophospholipids reduces the formation of adduct ions.

We next used a chemometric method based on COW (13, 14) for the alignment of high-resolution (Q-TOF) combined spectra before comparative analysis (Fig. 1E). We previously used COW to align mass spectra generated from direct infusion (13). Here, we used COW to align mass spectra generated from combined LC-separated total ion chromatograms. Next, ions of interest (e.g., those that are significantly altered in their intensities between the two conditions) are extracted for further analysis, such as the determination of peak area (Figs. 1E and 5D below). We validated the approach using pure standards in spiking experiments and found that the ion response was linear over biologically relevant ranges for a number of different lipids. During these standard additions, other prominent ions did not change significantly, illustrating the robust nature of the method with respect to the ionization characteristics of a lipid mixture (**Fig. 2A–D**). In addition, we found a high degree of reproducibility with respect to both retention time (Fig. 2E) and ion response (Fig. 2F, see supplementary Fig. IA–C).

Direct analysis of MAs in mycobacteria using HPLC-ESI-MS

The main motivation to develop the method presented here is based on applications of lipidomics for *i*) the discovery of novel lipid entities/pathways and *ii*) compara-
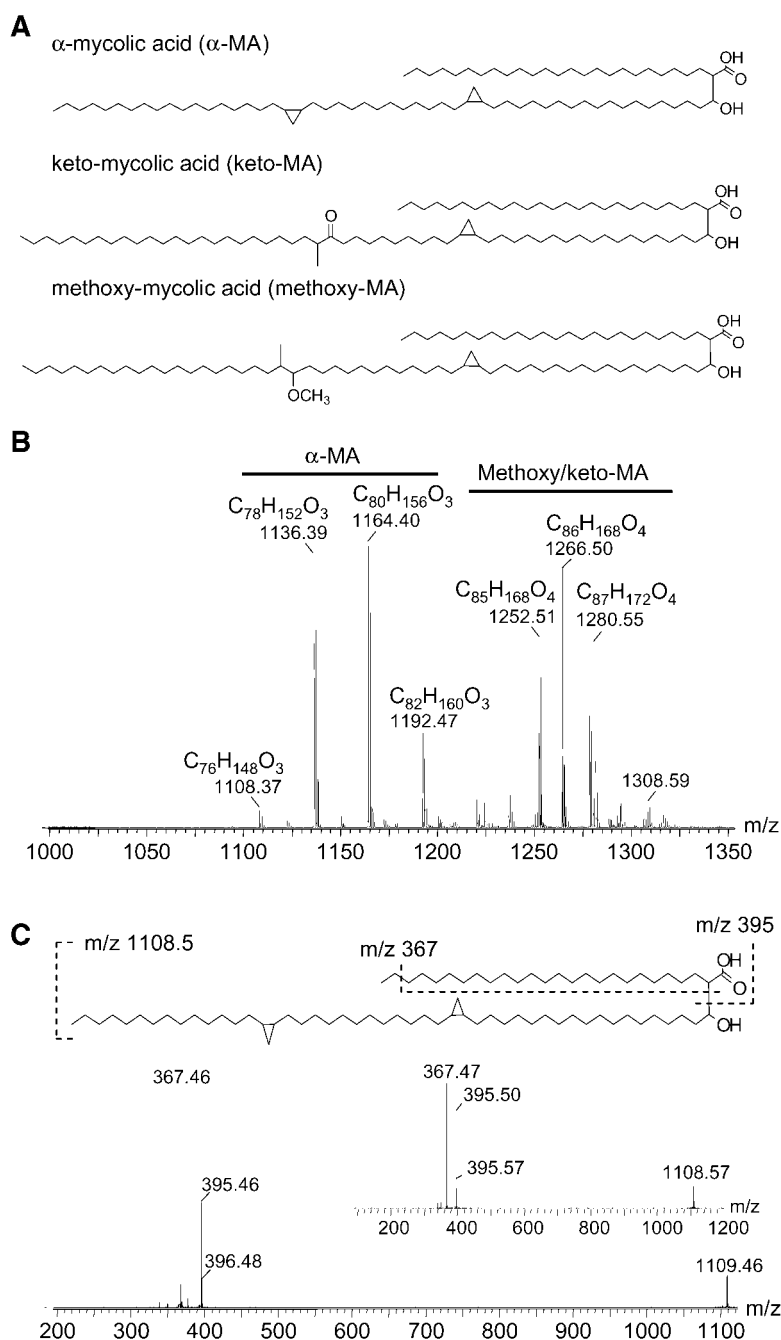

Fig. 3. Characterization of MAs derived from mycobacteria. A: Structures of α-MA, methoxy-MA, and keto-MA, the three major types of MAs in mycobacteria. B: MS profile of MA from *M. tuberculosis*. C: Product ion analysis (MS/MS) of *m/z* 1,108.5, an α-MA in extracts from *M. bovis* Bacille Camette-Guérin (BCG) (the inset displays MS/MS of ions obtained from a commercial standard).

tive analyses of components in lipid mixtures that have very diverse chemical compositions. One such example involves lipid extracts from mycobacteria that harbor an unusually diverse set of lipids in their membrane and cell wall (17, 18). In fact, the precise molecular structures of many of these lipids are still unknown, despite decades of biochemical analysis. Here, we used the method described above to analyze complex lipid mixtures from mycobacteria grown under different physiological conditions. As in the case of brain lipids (Fig. 1), LC-MS led to substantial signal enhancement of many prominent ions compared with direct sample introduction bypassing the column (data not shown). More importantly, because of low ion responses and isobaric interference, certain glycerophospholipids, menaquinones, MAs, and phosphatidylinositol mannosides, which range in mass from ∼1,000 to ∼2,500, were barely detected in mycobacterial extracts without chromatographic separation but could be qualitatively and semiquantitatively analyzed with our method (Fig. 1C and data not shown).

MAs are hydroxylated α-alkyl-β-hydroxy branched chain fatty acids that in mycobacteria contain 60–90 carbon atoms. They represent major cell envelope components and are either covalently linked to the cell wall arabinogalactan or form part of other esterified derivatives such as trehalose monomycolates and dimycolates (19, 20). MAs constitute the major mycobacterial hydrophobic barrier responsible for resistance to drugs and oxidative stress (21, 22) and furthermore play an active role in host-pathogen interactions (23) through host receptors (e.g., CD1 receptor and Galectin-3) (24). Surprisingly, subtle changes in the MA structure can have profound effects on the physiology and virulence of the tubercle bacillus (25–27). Not surprisingly, the biosynthetic machinery of MAs is an important target of antimycobacterial drugs (28–30).

MAs form a complex family of lipids and are categorized according to functional groups (e.g., cyclopropane, keto, and methoxy groups, numbers of double bonds in *cis* and *trans* configurations) in their meromycolate chains as well
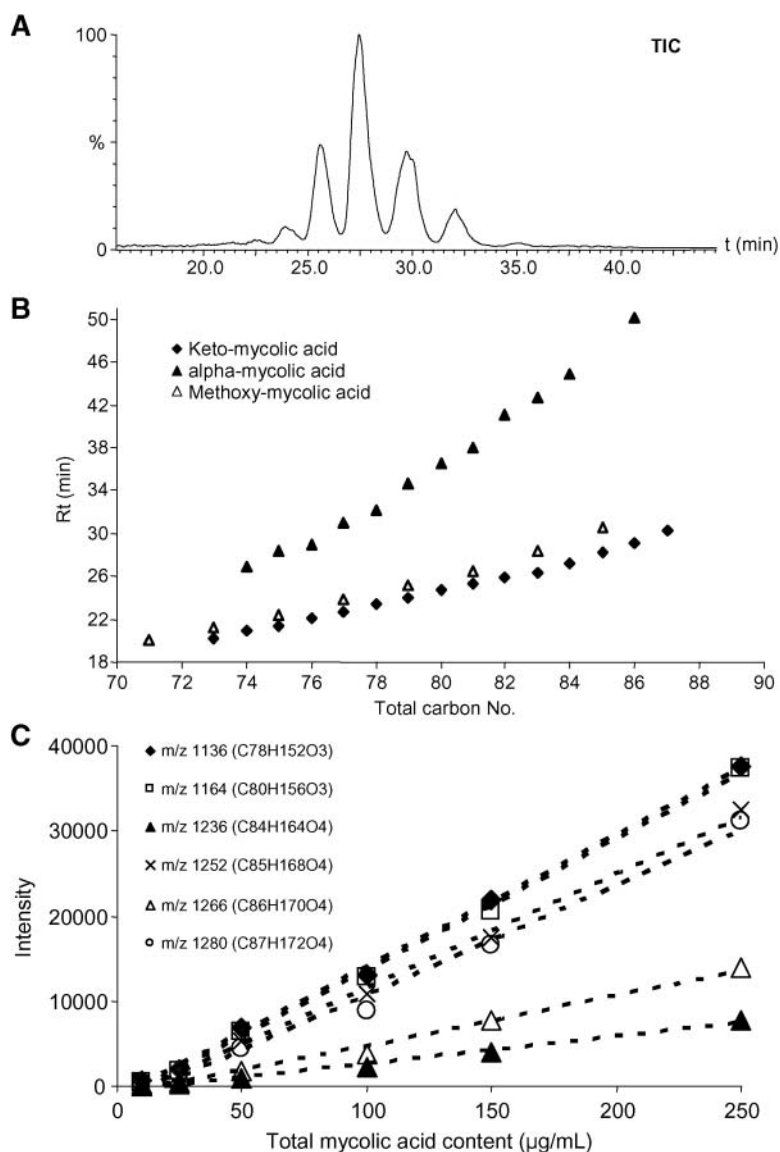

Fig. 4. HPLC analysis of MAs. A: Total ion chromatograms of MAs from *M. tuberculosis*. B: Elution times of selected major MAs in *M. tuberculosis*. Rt, retention time. C: MS signal intensities of different concentrations of the three major MA types show good linear responses.

Sensitive profiling of chemically diverse bioactive lipids 1981

as the number of carbon atoms (**Fig. 3A**). To date, for analysis of intact MA, methyl ester derivatization was applied followed by GC-MS (31) or matrix-assisted laser desorption ionization-TOF (32, 33). Here, crude lipid extracts or enriched fractions of intact MAs from *M. bovis* BCG and *M. tuberculosis* (a commercial sample from Sigma and a kind gift from Dr. John T. Belisle) were, for the first time, analyzed directly by LC-MS with excellent detection of ∼200 MAs and their derivatives (Figs. 3B, **4**, **5A**, **B** and data not shown). LC-MS/MS was next used to characterize the composition of MA, which upon collision-induced dissociation lost the α-branch as a (negatively charged) fatty

acyl. Fragmentation of m/z 1,108.5, an α-MA present in many species of mycobacteria including *M. bovis* BCG (Fig. 3C), yielded an identical pattern [i.e., fragment ions with m/z 395 (C_{26}) and m/z 367 (C_{24})] to that of a commercially available MA standard from *M. tuberculosis* (Fig. 3C, inset). These results are consistent with a molecular composition of $C_{76}H_{148}O_3$. We also investigated the potential of our method for semiquantitative analysis of MAs and found a smooth increase in the retention time of MA with increasing total carbon numbers (Fig. 4B) and a good linear response with increasing concentration (Fig. 4C) of mixtures with a total concentration of 10–250 µg/ml MAs.
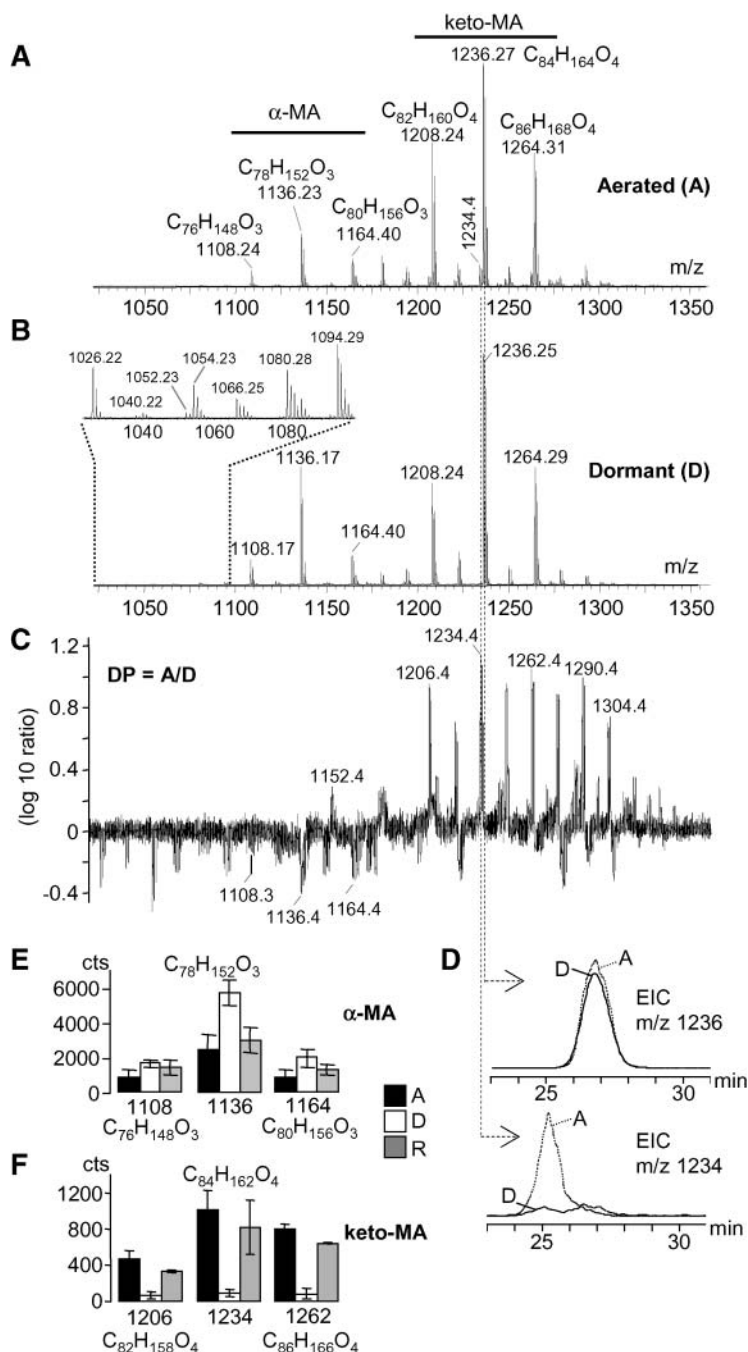
Fig. 5. Differential analysis of MAs from *M. bovis* Bacille Camette-Guérin (BCG) under different physiological conditions. A, B: MA profiles of *M. bovis* BCG cultivated in aerated stationary (A) and hypoxic dormancy (B) conditions. The inset in B illustrates the large number of ions that originate from MAs in addition to the well-characterized α-MA and keto-MA. C: The differential profile (DP) is a point-to-point comparison of combined spectra and displays ions with increased intensities (upward deflections) and ions with decreased intensities (downward deflections). D: Extracted ion chromatograms (EIC) of m/z 1,236 and 1,234. E, F: Semiquantitative analysis of MAs based on extracted ion chromatograms from bacterial extracts derived from aerated stationary (A), dormant (D), and resuscitated (R) cultures [n = 3, standard deviation (SD) indicated].

The limit of detection (signal/noise = 3) was estimated to be <10 pmol.

Profiling of MAs in *M. bovis* BCG under different physiological conditions

We next compared MAs from *M. bovis* BCG cultures that were grown under different physiological conditions. We focused on a widely used model system for nonreplicative dormancy induced by hypoxia (34). This model has gained substantial interest recently in the field of drug discovery because it allows the investigation of adaptation (and resuscitation) to (from) nonreplicative conditions. Such "dormant" bacilli are difficult to target with existing therapeutic interventions. MAs were liberated from delipidated cells by alkaline hydrolysis and extracted using diethyl ether. The spectra obtained from dormant cultures (D) were qualitatively similar to those from aerated stationary bacilli (A) (Fig. 5A, B). *M. bovis* BCG strains contain α-MAs similar to those found in *M. tuberculosis*, whereas the methoxy-MAs are very low abundant (Fig. 5) in *M. bovis* BCG and very high in *M. tuberculosis* (Fig. 3B). Differential analysis (Fig. 5C) shows a decrease in the major α-MA (*m/z* 1,108, 1,136, and 1,164) and a slight increase in most major keto-MAs (*m/z* 1,208, 1,236, and 1,264) in aerated cells (Fig. 5C, D). Interestingly, ions that correspond in *m/z* to minor forms of MAs, namely keto-MA (Fig. 5A) with an additional double bond (e.g., *m/z* 1,206, 1,234, and 1,262), are almost entirely eliminated upon entry into dormancy (Fig. 5D). This is observed for the whole series of keto-MAs and is reversed when bacteria are resuscitated with oxygen (Fig. 5E, F), indicating physiological adaptation.

The high sensitivity and resolution of this method will thus be an excellent tool for the analysis of changes in chemical fine structure and their relation to virulence and immune responses (25). For accurate quantification, synthetic stable isotope (internal) standards would be necessary, particularly if molecular species with different chain lengths are to be quantified (35). But even without the availability of such internal standards (which is the case for many if not most mycobacterial lipids), the analytical method described here can readily be applied in comparative and semiquantitative studies. Compared with alternative mass spectrometry-based methods for the detection of MAs, the present approach does not require any special sample processing, derivatization, or clean-up.

It is remarkable that a wide variety of complex lipids, including various MA derivatives, *N*-acetylated phosphatidylethanolamines, and menaquinones were successfully resolved and well detected using this method (Fig. 1C and data not shown). Multiple possible structures at the same *m/z* and isotopic interference are common problems in mass spectrometry-based lipidomics. Using upfront LC separation, some of these complications could be resolved for a number of lipids from different classes (see Fig. 1D for elution times of lipids). Tandem mass spectrometry (e.g., using selective parent-to-daughter transitions) will be a tool of choice to follow compounds of interest and to discriminate isobaric structures with the same chemical formula.

In conclusion, we describe an improved LC-MS-based method for the separation, characterization, and semiquantification of lipids from complex mixtures. The key novelty of this method is its wide applicability to lipid extracts of considerable chemical complexity (36). Polar membrane glycerophospholipids, cardiolipins, gangliosides, sphingolipids, and phosphatidylinositol mannosides as well as nonpolar components such as *N*-acetylated phosphatidylethanolamines, menaquinones, and MAs can be separated and analyzed in qualitative (e.g., by MS/MS) and (semi)quantitative ways in a single LC-MS experiment. **JLR**

REFERENCES

1. Kim, H. Y., T. C. Wang, and Y. C. Ma. 1994. Liquid chromatography/mass spectrometry of phospholipids using electrospray ionization. *Anal. Chem.* **66:** 3977–3982.
2. Han, X., and R. W. Gross. 1994. Electrospray ionization mass spectroscopic analysis of human erythrocyte plasma membrane phospholipids. *Proc. Natl. Acad. Sci. USA.* **91:** 10635–10639.
3. Pulfer, M., and R. C. Murphy. 2003. Electrospray mass spectrometry of phospholipids. *Mass Spectrom. Rev.* **22:** 332–364.
4. Hsu, F. F., and J. Turk. 2003. Electrospray ionization/tandem quadrupole mass spectrometric studies on phosphatidylcholines: the fragmentation processes. *J. Am. Soc. Mass Spectrom.* **14:** 352–363.
5. Taguchi, R., T. Houjou, H. Nakanishi, T. Yamazaki, M. Ishida, M. Imagawa, and T. Shimizu. 2005. Focused lipidomics by tandem mass spectrometry. *J. Chromatogr. B Analyt. Technol. Biomed. Life Sci.* **823:** 26–36.
6. Merrill, A. H., Jr., M. C. Sullards, J. C. Allegood, S. Kelly, and E. Wang. 2005. Sphingolipidomics: high-throughput, structure-specific, and quantitative analysis of sphingolipids by liquid chromatography tandem mass spectrometry. *Methods.* **36:** 207–224.
7. Sullards, M. C., E. Wang, Q. Peng, and A. H., Merrill, Jr. 2003. Metabolomic profiling of sphingolipids in human glioma cell lines by liquid chromatography tandem mass spectrometry. *Cell Mol. Biol.* **49:** 789–797.
8. Taguchi, R., J. Hayakawa, Y. Takeuchi, and M. Ishida. 2000. Two-dimensional analysis of phospholipids by capillary liquid chromatography/electrospray ionization mass spectrometry. *J. Mass Spectrom.* **35:** 953–966.
9. Hermansson, M., A. Uphoff, R. Kakela, and P. Somerharju. 2005. Automated quantitative analysis of complex lipidomes by liquid chromatography/mass spectrometry. *Anal. Chem.* **77:** 2166–2175.
10. Laaksonen, R., R. Laaksonen, M. Katajamaa, H. Paiva, M. Sysi-Aho, L. Saarinen, P. Junni, D. Lutjohann, J. Smet, C. R. Van, et al. 2006. A systems biology strategy reveals biological pathways and plasma biomarker candidates for potentially toxic statin-induced changes in muscle. *PLoS.* **1:** e97.
11. Wenk, M. R. 2005. The emerging field of lipidomics. *Nat. Rev. Drug Discov.* **4:** 594–610.
12. Dick, T., B. H. Lee, and B. Murugasu-Oei. 1998. Oxygen depletion induced dormancy in *Mycobacterium smegmatis*. *FEMS Microbiol. Lett.* **163:** 159–164.
13. Guan, X. L., X. He, W. Y. Ong, W. K. Yeo, G. Shui, and M. R. Wenk. 2006. Non-targeted profiling of lipids during kainate-induced neuronal injury. *FASEB J.* **20:** 1152–1161.

14. Nielsen, N. V., J. M. Carstensen, and J. Smedsgaard. 1998. Alignment of single and multiple wavelength chromatographic profiles for chemometric data analysis using correlation optimised warping. *J. Chromatogr. A.* **805:** 17–35.

15. Wenk, M. R., L. Lucast, P. G. Di, A. J. Romanelli, S. F. Suchy, R. L. Nussbaum, G. W. Cline, G. I. Shulman, W. McMurray, and C. P. De. 2003. Phosphoinositide profiling in complex lipid mixtures using electrospray ionization mass spectrometry. *Nat. Biotechnol.* **21:** 813–817.

16. Lytle, C. A., Y. D. Gan, and D. C. White. 2000. Electrospray ionization/mass spectrometry compatible reversed-phase separation of phospholipids: piperidine as a post column modifier for negative ion detection. *J. Microbiol. Methods.* **41:** 227–234.

17. Brennan, P. J. 2003. Structure, function, and biogenesis of the cell wall of *Mycobacterium tuberculosis*. *Tuberculosis (Edinb.).* **83:** 91–97.

18. Jain, M., C. J. Petzold, M. W. Schelle, M. D. Leavell, J. D. Mougous, C. R. Bertozzi, J. A. Leary, and J. S. Cox. 2007. Lipidomics reveals control of *Mycobacterium tuberculosis* virulence lipids via metabolic coupling. *Proc. Natl. Acad. Sci. USA.* **104:** 5133–5138.

19. Barry, C. E., III, R. E. Lee, K. Mdluli, A. E. Sampson, B. G. Schroeder, R. A. Slayden, and Y. Yuan. 1998. Mycolic acids: structure, biosynthesis and physiological functions. *Prog. Lipid Res.* **37:** 143–179.

20. Takayama, K., C. Wang, and G. S. Besra. 2005. Pathway to synthesis and processing of mycolic acids in *Mycobacterium tuberculosis*. *Clin. Microbiol. Rev.* **18:** 81–101.

21. Yuan, Y., R. E. Lee, G. S. Besra, J. T. Belisle, and C. E. Barry, III. 1995. Identification of a gene involved in the biosynthesis of cyclopropanated mycolic acids in *Mycobacterium tuberculosis*. *Proc. Natl. Acad. Sci. USA.* **92:** 6630–6634.

22. Daffe, M., and P. Draper. 1998. The envelope layers of mycobacteria with reference to their pathogenicity. *Adv. Microb. Physiol.* **39:** 131–203.

23. Nuzzo, I., M. Galdiero, C. Bentivoglio, R. Galdiero, and C. C. Romano. 2002. Apoptosis modulation by mycolic acid, tuberculostearic acid and trehalose 6,6′-dimycolate. *J. Infect.* **44:** 229–235.

24. Barboni, E., S. Coade, and A. Fiori. 2005. The binding of mycolic acids to galectin-3: a novel interaction between a host soluble lectin and trafficking mycobacterial lipids? *FEBS Lett.* **579:** 6749–6755.

25. Rao, V., F. Gao, B. Chen, W. R. Jacobs, Jr., and M. S. Glickman. 2006. Trans-cyclopropanation of mycolic acids on trehalose dimycolate suppresses *Mycobacterium tuberculosis* -induced inflammation and virulence. *J. Clin. Invest.* **116:** 1660–1667.

26. Liu, J., C. E. Barry, III, G. S. Besra, and H. Nikaido. 1996. Mycolic acid structure determines the fluidity of the mycobacterial cell wall. *J. Biol. Chem.* **271:** 29545–29551.

27. Glickman, M. S., J. S. Cox, and W. R. Jacobs, Jr. 2000. A novel mycolic acid cyclopropane synthetase is required for cording, persistence, and virulence of *Mycobacterium tuberculosis*. *Mol. Cell.* **5:** 717–727.

28. Smith, C. V., V. Sharma, and J. C. Sacchettini. 2004. TB drug discovery: addressing issues of persistence and resistance. *Tuberculosis (Edinb.).* **84:** 45–55.

29. Bhatt, A., L. Kremer, A. Z. Dai, J. C. Sacchettini, and W. R. Jacobs, Jr. 2005. Conditional depletion of KasA, a key enzyme of mycolic acid biosynthesis, leads to mycobacterial cell lysis. *J. Bacteriol.* **187:** 7596–7606.

30. Lin, T. W., T. W. Lin, M. M. Melgar, D. Kurth, S. J. Swamidass, J. Purdon, T. Tseng, G. Gago, P. Baldi, H. Gramajo, and S. C. Tsai. 2006. Structure-based inhibitor design of AccD5, an essential acyl-CoA carboxylase carboxyltransferase domain of *Mycobacterium tuberculosis*. *Proc. Natl. Acad. Sci. USA.* **103:** 3072–3077.

31. Stratton, H. M., P. R. Brooks, and R. J. Seviour. 1999. Analysis of the structural diversity of mycolic acids of Rhodococcus and Gordonia [correction of Gordonla] isolates from activated sludge foams by selective ion monitoring gas chromatography-mass spectrometry (SIM GC-MS). *J. Microbiol. Methods.* **35:** 53–63.

32. Laval, F., M. A. Laneelle, C. Deon, B. Monsarrat, and M. Daffe. 2001. Accurate molecular mass determination of mycolic acids by MALDI-TOF mass spectrometry. *Anal. Chem.* **73:** 4537–4544.

33. Fujita, Y., T. Naka, T. Doi, and I. Yano. 2005. Direct molecular mass determination of trehalose monomycolate from 11 species of mycobacteria by MALDI-TOF mass spectrometry. *Microbiology.* **151:** 1443–1452.

34. Boon, C., and T. Dick. 2002. *Mycobacterium bovis* BCG response regulator essential for hypoxic dormancy. *J. Bacteriol.* **184:** 6760–6767.

35. Koivusalo, M., P. Haimi, L. Heikinheimo, R. Kostiainen, and P. Somerharju. 2001. Quantitative determination of phospholipid compositions by ESI-MS: effects of acyl chain length, unsaturation, and lipid concentration on instrument response. *J. Lipid Res.* **42:** 663–672.

36. Fahy, E., E. Fahy, S. Subramaniam, H. A. Brown, C. K. Glass, A. H. Merrill, Jr., R. C. Murphy, C. R. Raetz, D. W. Russell, Y. Seyama, et al. 2005. A comprehensive classification system for lipids. *J. Lipid Res.* **46:** 839–861.